Oecologia (2004) 141: 373–384
DOI 10.1007/s00442-004-1647-7

ECOPHYSIOLOGY

Kenneth R. N. Anthony · Sean R. Connolly

Environmental limits to growth: physiological niche boundaries of corals along turbidity–light gradients

Received: 12 February 2004 / Accepted: 27 May 2004 / Published online: 20 August 2004

Abstract The physiological responses of organisms to resources and environmental conditions are important determinants of niche boundaries. In previous work, functional relationships between organism energetics and environment have been limited to energy intakes. However, energetic costs of maintenance may also depend on the supply of resources. In many mixotrophic organisms, two such resource types are light and particle concentration (turbidity). Using two coral species with contrasting abundances along light and turbidity gradients (*Acropora valida* and *Turbinaria mesenterina*), we incorporate the dual resource-stressor roles of these variables by calibrating functional responses of energy costs (respiration and loss of organic carbon) as well as energy intake (photosynthesis and particle feeding). This allows us to characterize physiological niche boundaries along light and turbidity gradients, identify species-specific differences in these boundaries, and assess the sensitivity of these differences to interspecific differences in particular functional response parameters. The turbidity-light niche of *T. mesenterina* was substantially larger than that of *A. valida*, consistent with its broader ecological distribution. As expected, the responses of photosynthesis, heterotrophic capacity, respiration, and organic carbon loss to light and turbidity varied between species. Niche boundaries were highly sensitive to the functional responses of energy costs to light and turbidity. Moreover, the study species' niche differences were almost entirely attributable to species-specific differences in one functional response: that of respiration to turbidity. These results demonstrate that functional responses of energy-loss processes are important determinants of species-specific physiological limits to growth, and thereby of niche differences in reef corals. Given that many resources can stress organisms when supply rates are high, we propose that the functional responses of energy losses will prove to be important determinants of niche differences in other systems as well.

Keywords Energy balance · Functional response · Irradiance · Scleractinian coral · Sediment

K. R. N. Anthony (✉) · S. R. Connolly
Centre for Coral Reef Biodiversity, School of Marine Biology and Aquaculture, James Cook University, Townsville, Queensland, 4811, Australia
e-mail: Kenneth.Anthony@jcu.edu.au

Introduction

In any species, the key fitness components of survival, growth and reproduction all depend on the availability of resources (e.g. energy) and environmental factors that directly or indirectly influence organism energy balance. In habitats characterized by resource limitation and/or harsh physico-chemical conditions, variation in the capacity to access and use resources, and to tolerate stress, may contribute strongly to the structuring of assemblages (Chesson and Huntly 1997; Emery et al. 2001). The link between the physiological processes underlying ecological performance and patterns of distribution and abundance of species along environmental gradients provides a mechanistic basis for predicting effects of environmental disturbances on populations and communities. In recent years, this concept has moved to the forefront of theoretical physiological and ecological research (Calow and Sibly 1990; Gurney et al. 1996; Maltby 1999; Kooijman 2000).

A useful framework within which to formulate the relationship between physiological processes and ecological performance is that of the physiological niche: the set of environmental conditions under which a species can persist (cf. Hutchinson 1957; Leibold 1995). Characterizing niche differences among species requires understanding how they respond to resources and environmental stressors. The relationship between resource levels and energy acquisition is typically quantified formally in terms of a functional response, with loss rates modeled as constant, per individual or per unit biomass (e.g. Sebens 1982, 1987; Leibold 1995; Brose et al. 2003). However, loss rates also depend on physico-chemical conditions, so

adapting the functional response approach to energy loss rates is important if we wish to characterize niche boundaries along environmental gradients. Indeed, many environmental factors that organisms use as resources also impose stresses, such as the availability of macronutrients to plants (e.g. Sultan and Bazzaz 1993), and the availability of light to primary producers in general (review by Falkowski and Raven 1997). In many cases, the functional responses of energy intake and loss processes are thus likely to trade off along a resource availability axis.

An ideal model system for investigating how differences in species' responses to resource-stress variables lead to differences in ecological distribution is that of photosymbiotic, scleractinian reef corals. This group naturally spans a broad range of environmental conditions, from clear oceanic waters to coastal habitats characterized by high concentrations of suspended sediment (Veron 1986), indicating a high degree of physiological or trophic diversity (Anthony and Fabricius 2000). Gradients in turbidity regime and light availability are often associated with a gradient in coral species composition (e.g. Done 1982, 1983), suggesting variation in the location of turbidity-light niche boundaries among coral species. Specifically, coral assemblages in high-sedimentation/high-turbidity habitats are often dominated by species different from those characteristic of low-turbidity habitats (e.g. Acevedo et al. 1989; McClanahan and Obura 1997). Functionally, such a pattern of varying dominance along environmental gradients is analogous to those observed for plant communities (e.g. Ohmann and Spies 1998; Emery et al. 2001; Seabloom et al. 2001).

Several mechanisms may explain an inshore-offshore gradient in species distributions. Firstly, tradeoffs in the efficiency of light use in low- versus high-light conditions may create partitioning along a light availability gradient, such as those found for plants in the forest canopy versus understorey (e.g. Chazdon et al. 1996) and as proposed by Porter (1976) for scleractinian corals. Secondly, coral species that perform well in high-turbidity areas may have greater heterotrophic capacity, and thus obtain more energy from organic suspended particles (Anthony and Fabricius 2000). If there is a physiological cost to this capacity, it may be favored in high-turbidity, but not in low-turbidity conditions. Alternatively, rates of respiration and organic carbon loss are also likely to be functions of turbidity, and clear-water species may exhibit greater sensitivity to increased turbidity than turbid-water species.

One way to assess the relative contribution of these metabolic processes to differences in species distributions is to calibrate functional responses for both energy intake and loss as functions of environmental variables (such as light and turbidity), and to combine those responses into an energy balance model. We can then use this model to determine species' physiological niche boundaries (conditions where the energy balance is zero), and to assess how sensitive those niche boundaries are to the parameters that characterize how photosynthesis, heterotrophy, respiration, and organic carbon loss respond to environmental variables.

In this study, we model limits to growth and survival in symbiotic reef corals as functions of light availability and particle concentration (turbidity). Firstly, we calibrate functional responses of respiration and organic carbon loss (e.g. as mucus excretion) to irradiance and turbidity using two coral species with contrasting distribution patterns along turbidity gradients. Secondly, we predict the location of physiological niche boundaries by calculating energetic zero-growth isoclines for the two species. Using these energy-balance isoclines, we assess (1) whether the inshore dominant has a broader niche than the generalist, (2) the sensitivity of niche boundaries to different functional response parameters, and (3) the contribution of different functional responses to these niche differences.

Materials and methods

Energy balance model

To estimate the location of limits for long-term coral growth and survival within light-turbidity niche space, we formulate an energy-budget model in which both intake and cost rates are functions of irradiance (I) and particle concentration (turbidity, γ). For simplicity, we use daily average rather than instantaneous irradiance as it can be shown that integration of the photosynthesis-irradiance model over the day can be approximated by the average hourly rate multiplied by the number of daylight hours (Appendix 1). Energy balance (E_B) or scope for growth (see also Maltby 1999) is given by

$$E_B = P(I,\gamma) + H(\gamma) - R(I,\gamma) - L(I,\gamma), \quad (1)$$

where P, H, R, and L represent daily rates of photosynthesis, heterotrophy, respiration, and organic carbon loss, respectively. The combinations of I and γ for which $E_B = 0$ are light-turbidity niche boundaries: thresholds below which long-term survival is impossible, because energy expenditure exceeds energy acquisition.

Respiration

Most previous energy-balance studies of corals have used rate of respiration as a constant (e.g. Barnes and Chalker 1990) and assumed it to equal the rate of dark respiration. However, above some basal rate of maintenance metabolism, organism respiration is likely to be a function of the level of activity or stress imposed by the environment (e.g. Withers 1992), such as particle concentration (turbidity) and associated sediment cleaning in corals (e.g. Riegl and Branch 1995). Ignoring, for the time being, potential interactive effects of light and turbidity, rates of respiration along a light-turbidity gradient can be modelled as

$$R(\gamma, I) = R_{\text{base}} + R(\gamma) + R(I), \tag{2}$$

where R_{base} is dark respiration in clear water (a constant), $R(I)$ is the functional response of respiration to light, and $R(\gamma)$ is the functional response of respiration to turbidity. To characterize $R(\gamma)$, we use a simple model that can approximate a range of qualitatively different functional responses:

$$R(\gamma, I) = R_{\text{base}} + R_\gamma \left(\frac{\gamma}{\gamma_{\max}}\right)^{a_{R_\gamma}} + R(I), \tag{3}$$

where R_γ is turbidity-induced rate of respiration and a_{R_γ} is a dimensionless exponent. Turbidity, γ, is non-dimensionalized to a reference turbidity level, $\gamma_{\max}$ which insures that the unit of R_γ is energy (or carbon) per unit time. When $R_\gamma \approx 0$, the metabolic cost of coping with turbidity is negligible. When $a_{R_\gamma} = 1$, then the functional response to turbidity is linear (i.e., metabolism increases proportionately with particle concentration). When $a_{R_\gamma} < 1$, the response of respiration rate to turbidity diminishes as turbidity increases. We would expect this functional response if there is a maximum rate of sediment removal, and corals approach this maximum for realistic sediment loads. Conversely, it is possible that the cost of removing a unit of sediment increases as sediment load increases ($a_{R_\gamma} > 1$), in which case respiration rate will be an accelerating function of turbidity.

Because net photosynthesis (P_{net}) response curves are generally formulated in a way that the parameters I_k and $P_{\max}$ (see below) implicitly account for light-enhanced respiration (Chalker et al. 1983; Barnes and Chalker 1990), we here explicitly characterize $R(\gamma)$, but we model $R(I)$ implicitly as part of net photosynthesis (see Photosynthesis and heterotrophy, below).

Organic carbon loss

Previous studies of organic carbon losses in corals have focused mainly on comparisons of loss rates at low versus high sediment loads (Riegl and Branch 1995) or at low versus high irradiance (Crossland 1987). Accordingly, little is known about the form of the functional response of carbon loss to turbidity or irradiance. We expect the rate of organic carbon loss (L) to be a function of two major processes. Firstly, mucus production will increase in response to the physical stress of turbidity and sediment deposition onto coral tissues, mainly as a sediment rejection response (e.g. Riegl and Branch 1995) or perhaps to facilitate particle feeding (Anthony 1999). Secondly, high rates of organic carbon loss may indicate nutrient-limited growth at high irradiances as more carbon is being fixed photosynthetically than can be incorporated into proteins and lipids (e.g. Muscatine 1990). Following Eq. 3, we model rates of organic carbon loss according to:

$$L(\gamma, I) = L_{\text{base}} + L_\gamma \left(\frac{\gamma}{\gamma_{\max}}\right)^{a_{L_\gamma}} + L_I (I I_{\max})^{a_{L_I}}, \tag{4}$$

where L_{base}, L_γ, and a_{L_γ} are analogous to R_{base}, R_γ, and a_{R_γ} from Eq. 3. Similarly, the additional parameters L_I, $I_{\max}$, and a_{L_γ} account for the response of carbon losses to irradiance. As with Eq. 3, the functional form of this model is flexible enough to approximate both linear and non-linear functional responses.

Photosynthesis and heterotrophy

To complete the energy balance model given by Eq. 1, we utilize the functional responses of energy intake from photosynthesis (for review see Falkowski and Raven 1997; Lambers et al. 1997) and heterotrophy (e.g. Ferrier-Pages et al. 1998; Anthony 1999). Because rates of respiration (Eq. 3) and photosynthesis are assayed together using whole-colony respirometry, we express these as net rate of photosynthesis

$$P_{\text{net}}(I, \gamma) = P_{\text{gross}}(I, \gamma) - R(I, \gamma), \tag{5}$$

where $P_{\text{gross}}(I,\gamma)$ is gross rate of photosynthesis and $R(I,\gamma)$ is total rate of respiration. As mentioned above, however, gross photosynthesis and the light-enhanced component of respiration, $R(I)$, are typically estimated together:

$$P_{\text{gross}}(I, \gamma) - R(I) = P_{\max} \tanh\left(\frac{I}{I_k}\right). \tag{6}$$

Therefore, we combine Eqs. 2, 3, and 6 to model net photosynthesis as follows:

$$P_{\text{net}}(I, \gamma) = P_{\max} \tanh\left(\frac{I}{I_k}\right) - R_{\text{base}} - R_\gamma \left(\frac{\gamma}{\gamma_{\max}}\right)^{a_{R_\gamma}}. \tag{7}$$

Like higher plants and algae, corals photoacclimate by adjusting their photosynthetic parameters, $P_{\max}$ and I_k, to the light regime: both parameters tend to increase as growth irradiance increases (Chalker et al. 1983). To account for this, we expressed subsaturation irradiance (I_k) and maximum rate of photosynthesis ($P_{\max}$) as functions of daily average irradiance (assuming stable conditions) according to the photoacclimatory model of Anthony and Hoegh-Guldberg (2003a):

$$I_k(I) = I_{k\text{MS}} (I / I_{\max})^{\beta_1}, \tag{8a}$$

$$P_{\max}(I) = P_{\text{MS}} (I / I_{\max})^{\beta_2}, \tag{8b}$$

where $I_{k\text{MS}}$ is the maximum I_k value and P_{MS} is the

maximum P_{max} at the maximum environmental irradiance (I_{max}), and β_1 and β_2 are constants.

Coral heterotrophy can often be described by linear response curves at low to moderate plankton or particle concentrations (e.g. Ferrier-Pages et al. 1998; Anthony 1999). Over a wide range of particle concentrations, however, rate of heterotrophy is more generally described by a type-2 functional response

$$H(\gamma) = c_{org}\tau\varepsilon\frac{F_{max}\gamma}{\gamma + \gamma_{sat}}, \quad (9)$$

where c_{org} is the energy content of organic carbon, τ is the proportion of time feeding, ε is the assimilation efficiency, F_{max} is the maximum rate of ingestion, and γ_{sat} is the particle concentration at which the ingestion rate is half of maximum. Here, we assume that both feeding time and assimilation efficiency are a constant 50% (Anthony 1999) and that the organic content of particles is 5%. These estimates are towards the high end of the realistic range for natural turbidity regimes, thus the contribution of heterotrophy to the energy balance is likely to be overestimated. This makes our model conservative with respect to the hypothesis that heterotrophic feeding makes a minor contribution to the coral energy balance (Anthony and Fabricius 2000).

Study species and coral collecting

To compare niche boundaries among coral species that occur naturally in different types of sediment regimes, we selected two species: one that dominates subtidal areas of inshore, turbid reefs (*Turbinaria mesenterina*) and one that is widespread across inshore and offshore habitats in the Great Barrier Reef lagoon (*Acropora valida*). *T. mesenterina* forms large foliaceous stands in turbid water and tolerates severe sediment events. Although present in low-turbidity mid-shelf habitats, it is rarely found in high abundance there (Done 1982). *A. valida* is a branching (corymbose) species occurring mainly on reef crests on midshelf and offshore reefs, but also reaches high abundances in inshore, subtidal areas (K.R.N. Anthony, unpublished). Small colonies (recent recruits measuring 8–

Table 1 Variables used in energy balance model

Symbol	Unit	Interpretation
Parameters		
a_{R_γ}	Dimensionless	Exponent for turbidity-enhanced respiration
a_{L_γ}	Dimensionless	Exponent for turbidity-enhanced loss of organic carbon
a_{L_I}	Dimensionless	Exponent for light-enhanced loss of organic carbon
β_1	Dimensionless	Exponent relating I_k to I (at steady state)
β_2	Dimensionless	Exponent relating P_{max} to I (at steady state)
c_{org}	μg C μg $^{-1}$	Organic carbon content
ε	Dimensionless	Assimilation efficiency
I_k	μmol m^{-2} s^{-1}	Sub-saturation irradiance
I_{kMS}	μmol m^{-2} s^{-1}	Maximum I_k at steady-state irradiance
τ	Dimensionless	Proportion of time feeding
γ_{sat}	mg l^{-1}	Turbidity (concentration of suspended particles) at which particle feeding rate is half saturated
State variables		
E_B	μg C cm^{-2} d^{-1}	Energy balance
F_{max}	μg particles cm^{-2} d^{-1}	Maximum feeding (ingestion) rate
H	μg C cm^{-2} d^{-1}	Rate of heterotrophic energy intake
I	μmol m^{-2} s^{-1}	Average daily irradiance
I_{max}	μmol m^{-2} s^{-1}	Average, daily surface irradiance
L_{base}	μg C cm^{-2} d^{-1}	Basal rate of organic carbon loss
L_γ	μg C cm^{-2} d^{-1}	Turbidity-enhanced rate of organic carbon loss
L_I	μg C cm^{-2} d^{-1}	Light-enhanced rate of organic carbon loss
L	μg C cm^{-2} d^{-1}	Daily rate of organic carbon loss
P_g	μg C cm^{-2} d^{-1}	Daily rate of gross photosynthesis
P_{max}	μg C cm^{-2} d^{-1}	Maximum rate of gross photosynthesis
P_{MS}	μg C cm^{-2} d^{-1}	Maximum P_{max} at steady-state irradiance
$R(\gamma)$	μg C cm^{-2} d^{-1}	Rate of respiration as a function of turbidity
R_{base}	μg C cm^{-2} d^{-1}	Basal rate of respiration
R_γ	μg C cm^{-2} d^{-1}	Turbidity enhanced rate of respiration
R	μg C cm^{-2} d^{-1}	Daily rate of respiration
γ	mg l^{-1}	Concentration of suspended particles (turbidity)

10 cm diameter) were collected in Nelly Bay at Magnetic Island (Townsville). They were fixed individually to stands, each consisting of a PVC ring (7 cm diameter, 2 cm high) with holes to allow attachment and water flow past the base of the colony. To allow recovery from handling, they were left on racks in situ for 4 weeks. The corals were then transported to the Marine Aquarium Research Facilities Unit at James Cook University and kept at light, temperature and salinity conditions representative of those in their native habitat. Daily average irradiance in the tanks approximated 200 μmol m^{-2} s^{-1} (corresponding to 1200 hours maxima of 300–400 μmol m^{-2} s^{-1}) and was provided by metal halide lamps (400 W, EYE, Japan) programmed to follow a 12 h:12 h light:dark cycle. The temperature was kept at 26–27°C, salinity at 34.5–36.0 ppm, and the concentration of suspended particles was <2 mg l^{-1}.

Experimental design

Photoacclimation responses (Eq. 8a, Eq. 8b) and functional responses for heterotrophy (Eq. 9) were parameterized from published values (Table 1). To determine functional responses for net photosynthesis (photosynthesis–respiration) and organic carbon loss, we conducted two series of experiments under a wide range of turbidity levels (1–200 mg l^{-1}, γ_{max}) exposed to 4–6 light conditions (0–900 μmol photons m^{-2} s^{-1}, I_{max}). These levels span the range of particle concentrations and irradiances observed in coastal benthic habitats (e.g. Larcombe et al. 1995; Anthony et al. 2004). The sediment consisted of natural fine sediment (grain size <50 μm) collected from the sediment surface at the study site. To assay rates of organic carbon loss under varying particle loads, the sediment was combusted at 450°C for 4 h to remove any organic matter. Irradiance was produced by metal halide lamps (each 400 W, EYE, Japan) suspended at varying heights above the chambers. To normalize data to colony surface area, all colonies (and a ruler for scale) were photographed from above and from the side using a digital camera (Sony DSC-P1). Surface areas were determined from the digital images using the software package Mocha (Jandel Scientific).

Photosynthesis and respiration

The responses of photosynthesis and respiration to irradiance and turbidity were estimated by fitting Eq. 7 to observed net rate of photosynthesis for 4–6 levels of irradiance and turbidity using approximately 20 colonies per coral species. Oxygen respirometry runs were conducted using a system of six closed (re-circulating) flumes (2.7-l) fitted with oxygen electrodes connected to a logger (see Anthony and Hoegh-Guldberg 2003b). The flow was set to approximately 5–6 cm s^{-1} (determined by particle tracking) to facilitate oxygen exchange and to keep particles in suspension. The system was submerged in a jacket of running seawater to buffer temperature fluctuations and to allow periodic flushing of chambers (3-min flushing between every 27-min recording period). Irradiance was adjusted by elevating or lowering the lamps over the chambers, starting with an estimate of dark respiration in the morning. Each respirometry run was conducted over a 12-h period during which one sediment concentration was maintained in each chamber, whereas irradiance levels were increased every 2–3 h. Irradiance was measured at the level of the corals (accounting for turbidity) using a cosine corrected sensor (GaAsp photodiode, Hamamatsu, Japan). Particulate matter was delivered to the chambers by peristaltic pumps during the flushing periods. The particle concentration in each flume was determined by sampling 200 ml of water (during flushing periods) at 1–2 h intervals. Samples were filtered through pre-weighed GF/C filters, rinsed in distilled water and dried till constant weight. To control for photosynthesis and respiration of biofilm and micro-organisms, at least one chamber in each run was left empty.

Rate of organic carbon loss

To determine the functional relationship between particle concentration, irradiance and rate of organic carbon loss we used a technique modified from that of Crossland (1987) in which particulate and dissolved organic carbon lost from the corals was captured by filtration and analyzed quantitatively. The incubation system consisted of five sets of 15 open aquaria (3 l each) placed under metal-halide lamps (see above). Analogous to the respirometry runs, corals were exposed to 4–6 particle concentrations (ranging from 1 to 200 mg l^{-1}) and four irradiances (0, 100, 200 and 300 μmol photons m^{-2} s^{-1}) for 10–12 h. To minimize dissolved organic carbon in the incubation water, the seawater was pre-filtered through a canister filter (1 μm pore size) saturated with 10 g of pre-combusted (450°C) filter agent (Celite, Sigma). After each run, the corals were lifted out of their chambers, rinsed of adhering particles and mucus, and photographed for later analysis of surface areas. To determine all organic carbon in the incubation water and particles associated with each colony, approximately 3 g of pre-combusted Celite was added to each container and the water then filtered through two to three pre-combusted GF/C filters. To minimize loss of mucus and lipids due to oxidation and degradation, the samples were frozen immediately at −40°C and stored until analysis. Analyses were conducted using a CHN analyzer (Shimatzu 5000).

Calibration of functional responses

Photosynthesis and respiration rates obtained from the experiments were fitted to Eq. 7, and organic carbon loss rates were fitted to Eq. 4, using non-linear, least-squares estimation (STATISTICA 2001). This tested for the existence of a functional response (coefficients R_γ, L_γ,

and L_I not equal to zero), and yielded parameter estimates and associated standard errors. Functional responses were tested for nonlinearity (exponents not equal to unity) by comparing models with versus without power exponents using the Likelihood Ratio Statistic. The normalization constants γ_{max} and I_{max} were fixed at the maximum experimetal turbitidy (200 mg l^{-1}) and irradiance (900 µmol m^{-2} s^{-1}) levels.

Isocline analysis

Parameter estimates from the best-fit models of photosynthesis and respiration (Eq. 7) and organic carbon loss (Eq. 4), along with published parameter estimates for photoacclimation and heterotrophy, were used to estimate the location and behavior of niche boundaries (combinations of light and turbidity for which E_B=0 in Eq. 1) for each species. Niche boundaries were defined as turbidity and light conditions at which the energy balance (E_B) equals zero. Confidence limits around niche boundaries were estimated by Monte Carlo simulation (see Appendix 2).

To investigate the effect of varying strength of energy-cost functions to turbidity on the breadth of the physiological niche, we analyzed the sensitivity of niche boundaries to perturbations in turbidity-enhanced respiration and turbidity-enhanced organic carbon loss. This enabled us to assess the role of energy efficient strategies for handling sediment—i.e. cost-efficient removal of particles and minimal production of mucus sheets. Specifically, we compared the locations of niche boundaries under three main scenarios: (1) full model, (2) R_γ=0 (no functional response of respiration to turbidity), and (3) L_γ=0 (no functional response of organic carbon loss to turbidity). (Because our focus was the behavior of niche boundaries under low-light and high-turbidity conditions, perturbations of the organic carbon loss response to irradiance, L_I, was of secondary importance.) To examine the relative roles of heterotrophy and phototrophy in determining the location of niche boundaries, we compared two additional scenarios: H=0, and a 10% decrease in P_{max}. The scenario H=0 represents conditions under which polyps are permanently contracted and/or the particulate matter has minimal organic content, and a reduction in P_{max} mimics partial loss of symbionts

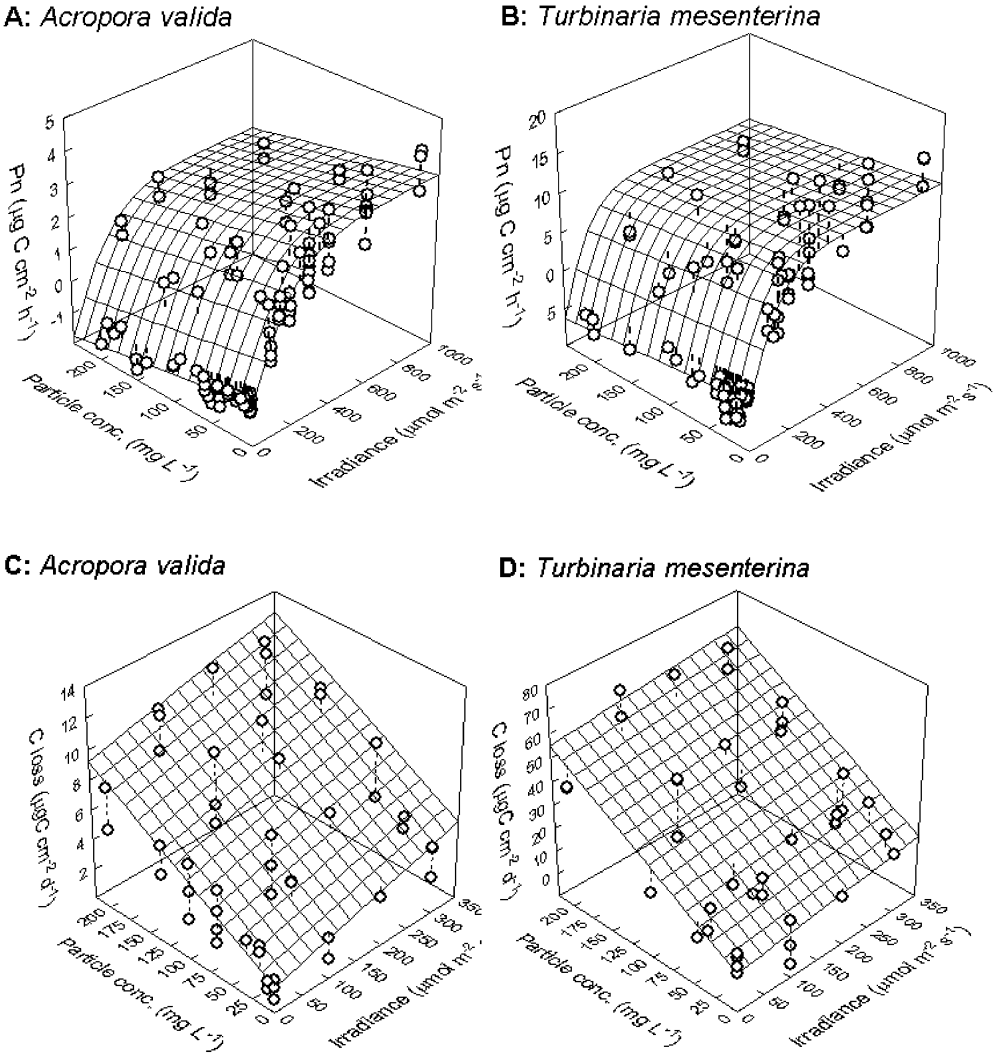

Fig. 1a–d Net rates of photosynthesis (gross photosynthesis–respiration) in (**a**) *A. valida* and (**b**) *T. mesenterina*, and rates of organic carbon loss in (**c**) *A. valida* and (**d**) *T. mesenterina* as a function of irradiance (daily averages) and concentration of fine suspended particles. Equation 6 was fitted to the net photosynthesis data, using a linear function for the response of respiration to turbidity (Table 2). Equation 4 was fitted to the data on organic carbon loss, using a linear function for the response to turbidity and irradiance (Table 2). The respiration response was assayed as part of the net photosynthesis response in order to account for interactions between light and turbidity, and (implicitly) for light-enhanced respiration. See Table 3 for parameter estimates. Note different scales on z-axes

(bleaching) or a reduction in photosynthetic capacity. Setting P_{max} to zero would not be meaningful as photosynthesis is the primary component of the energy budget of most photosymbiotic corals (Muscatine 1990; Anthony and Fabricius 2000).

Results

Functional responses: photosynthesis and respiration

Over the experimental range of particle concentrations (1–200 mg l^{-1}), rate of respiration more than doubled in *A. valida* (~130% above R_{base}) whereas respiration in *T. mesenterina* increased by approximately 65%. This is apparent as a decrease in net photosynthesis with increasing sediment concentration, with *A. valida* exhibiting a steeper decline than *T. mesenterina* (Fig. 1a, b). These results suggest that *T. mesenterina* is metabolically less sensitive to turbidity than *A. valida*. The function for net rate of photosynthesis (Eq. 7), in which a linear function was used for the respiration term (Eq. 3 with $a_{R_\gamma} = 1$), provided a good fit to the data in both species (more than 90% explained variation, with residuals distributed normally and exhibiting no evidence of bias). Moreover, the Likelihood Ratio Test failed to reject the linear model in favor of the (more parameterized) non-linear model (Table 2a). Therefore, the linear model was used in our niche boundary analysis.

The basal rate of respiration (R_{base}) of *T. mesenterina* (42±4.1 μg C cm^{-2} d^{-1}) was 4 times higher than that of *A. valida* (8.2±0.9 μg C cm^{-2} d^{-1}), reflecting baseline differences in biomass and physiological activity per unit surface area of the two species (Table 3). Also, the maximum rate of photosynthesis (P_{max}) per unit surface area of *T. mesenterina* (182±7.2 μg C cm^{-2} d^{-1}) was nearly 4 times higher than that of *A. valida* (43±8.2 μg C cm^{-2} d^{-1}) for the specific photoacclimative state of the experimental population (*I*~200 μmol photons m^{-2} s^{-1}). This observed difference in P_{max} between the study species is consistent with the difference in maximum photosynthetic capacity (P_{MS}) between *T. mesenterina* (Anthony and Hoegh-Guldberg 2003a) and seven species of *Acropora* (Chalker et al. 1983). Because P_{max} increases negligibly with irradiance above 200 μmol m^{-2} s^{-1} (Anthony and Hoegh-Guldberg 2003a), we used the experimental values of P_{max} as estimates of P_{MS} in the subsequent energy-balance analyses.

Observed differences in sub-saturation irradiances (I_k) between *A. valida* (251±mol m^{-2} s^{-1}) and *T. mesenterina* (±165 mol m^{-2} s^{-1}) in this study, however, were the opposite of published differences in maximum I_k(I_{kMS}) between *Acropora* sp. (181 μmol m^{-2} s^{-1}, Chalker et al. 1983) and *T. mesenterina* (373 μmol m^{-2} s^{-1}, Anthony and Hoegh-Guldberg 2003a), most likely due to differences in methodology. In this study, colonies of *A. valida* were illuminated directly from above, whereas in the study by Chalker et al. (1983) individual coral branches were illuminated from both sides. The I_k values produced in this study thus account for self-shading and are more representative of the ambient irradiance regime of whole coral colonies. To be consistent with our approach for P_{MS} above, we used the experimental I_k values of this study as estimates of I_{kMS} in subsequent energy-balance analyses (Table 4).

Table 2 Test of linearity of the functional responses of respiration to turbidity and of organic carbon loss to turbidity and irradiance (Eq. 3 and 7). The test statistic (Likelihood Ratio Statistic) was evaluated against the χ^2 distribution with degrees of freedom (*df*) being the difference in number of parameters between the two models. A non-significant result favors the simpler model (i.e. failure to reject the simple model in favor of the more parameterized model)

Response	Species	*n*	LRS	*df*	*P*	
A: Respiration	*T. mesenterina*	104	2.83	1	0.092	NS
	A. valida	125	0.10	1	0.750	NS
B: Organic carbon loss	*T. mesenterina*	39	0.79	2	0.672	NS
	A. valida	49	1.84	2	0.399	NS

Functional responses: organic carbon loss

The response of organic carbon loss to turbidity was slightly stronger in *T. mesenterina* than in *A. valida*. Specifically, over the experimental turbidity range, daily rates of organic carbon loss increased more than 4 times in *A. valida* (450% above L_{base}) and almost 5 times in *T. mesenterina* (480% above L_{base}, Fig. 1c, d). The response to turbidity was 4 times stronger than the response to light in both species, as indicated by the ratio of L_γ to L_I (Table 3). Overall, however, organic carbon losses accounted for approximately 10% of the total carbon loss (daily rates of respiration and organic carbon loss) at low turbidity and low light, and approximately 25% at maximum turbidity and light levels. Consistent with the pattern for respiration, the basal rates of organic carbon loss of *T. mesenterina* was more than 3 times higher than that of *A. valida*.

The linear functional responses (Eq. 4 with $a_{I_\gamma} = 0$, $a_{I_\gamma} = 0$) provided good fits to the data, explaining more than 80% of the variation (Table 3) and with residuals exhibiting no evidence of bias. Moreover, as in the respiration analysis, the Likelihood Ratio Test failed to reject the linear model in favour of the (more parameterized) non-linear model (Table 2). Accordingly, the exponents a_{L_γ} and a_{L_I} of the functional response were fixed to unity for the niche boundary analyses (see below).

Physiological niche boundaries

Predictions of the location of zero-growth (energy balance) isoclines and their confidence limits, based on Monte Carlo simulations, are presented in Fig 2a.

Table 3 Results of non-linear regression analyses of net rate of photosynthesis (gross rate of photosynthesis–rate of respiration) and rate of organic carbon loss in response to turbidity (1–200 mg l^{-1}) and irradiance (0–900 μmol m^{-2} s^{-1}), and rate of organic carbon loss in response to light and turbidity. Because Likelihood Ratio Tests supported the linear functional responses, the exponents $(a_{R_\gamma}, a_{L_\gamma}, a_{L_I})$ were fixed to unity. P_{max}, R_{base} and R_γ are converted to daily rates from data in Fig. 1a, b (see also Appendix 2)

Model	Variable	*A. valida*			*T. mesenterina*		
		Estimate	SE	R^2	Estimate	SE	R^2
A: Net photosynthesis	P_{max} (μg C cm^{-2} d^{-1})	43	8.2	0.92	185	7.2	0.91
	I_k (μmol m^{-2} s^{-1})	251	18		165	16	
	R_{base} (μg C cm^{-2} d^{-1})	8.2	0.88		42	4.1	
	R_γ (μg C cm^{-2} d^{-1})	10.4	1.6		38	8.6	
B: Organic carbon loss	L_{base} (μg C cm^{-2} d^{-1})	1.6	0.38	0.81	6.9	2.6	0.81
	L_γ (μg C cm^{-2} d^{-1})	8.2	0.61		40	3.8	
	L_I (μg C cm^{-2} d^{-1})	1.6	0.54		8.3	3.5	

Table 4 Summary of parameter values used in analyses of energy balance as a function of turbidity and irradiance in *A. valida* and *T. mesenterina*. Published data on feeding and photosynthesis for other members of the genus *Acropora* were used in lieu of such data for *A. valida*. (See Table 1 for units)

Parameter	Species	Estimate	SE	Source
I_{kMS}	*A. valida*	251[a]	18	This study
	T. mesenterina	165[a]	16	
P_{MS}	*A. valida*	43[a]	1.5	This study
	T. mesenterina	185[a]	7.2	
β_1	*Acropora* sp.	0.35	0.06	Chalker et al. (1983)
	T. mesenterina	0.34	0.05	Anthony and Hoegh-Guldberg (2003a, b)
β_2	*Acropora* sp.	0.08	0.06	Chalker et al. (1983)
	T. mesenterina	0.09	0.05	Anthony and Hoegh-Guldberg (2003a, b)
R_{base}	*A. valida*	8.2	0.91	This study
	T. mesenterina	42	4.1	
R_γ	*A. valida*	10	1.6	This study
	T. mesenterina	38	8.5	
L_{base}	*A. valida*	1.6	0.38	This study
	T. mesenterina	6.9	2.6	
L_γ	*A. valida*	8.2	0.61	This study
	T. mesenterina	40	3.8	
L_I	*A. valida*	1.6	0.54	This study
	T. mesenterina	8.3	3.5	
F_{max}	*A. millepora*	360[b]	120	Anthony and Fabricius (2000)
	T. mesenterina	1200	192	Anthony (unpublished)
τ	*A. valida*	0.50[c]	NA	Anthony (1999), Anthony and Fabricius (2000)
	T. mesenterina		This study	
γ_{sat}	*A. millepora*	>30[d]	NA	Anthony and Fabricius (2000)
	T. mesenterina	~50[d]	NA	Anthony (unpublished)
ε	*A. millepora*	0.50[e]	0.20	Anthony (1999), Anthony and Fabricius (2000)
c_{org}	NA	0.05	0.01	Anthony and Fabricius (2000)

[a] Assumes that I_k and P_{max} approximate I_{kMS} and P_{MS} for irradiances above 200 μmol m^{-2} s^{-1}

[b] Estimated as the maximum feeding rate within a turbidity range of 1–30 mg l^{-1} (converted from hourly rates of 15 and 50 μgC cm^{-2} h^{-1}, respectively). Values are thus likely to provide underestimates at higher particle concentrations. SEs are based on sample variation at 30 mg l^{-1}

[c] Based on observations that most coral species (including the study species) feed mainly at night

[d] Parameter could only be estimated with low precision because of relatively narrow turbidity ranges (<50 mg l^{-1}) and the SE is therefore omitted—i.e. the variance contribution from heterotrophy is likely to be underestimated

[e] ε decreases with ingestion rates so a value of 0.5 will represent an underestimate at low turbidity and an overestimate at high turbidity

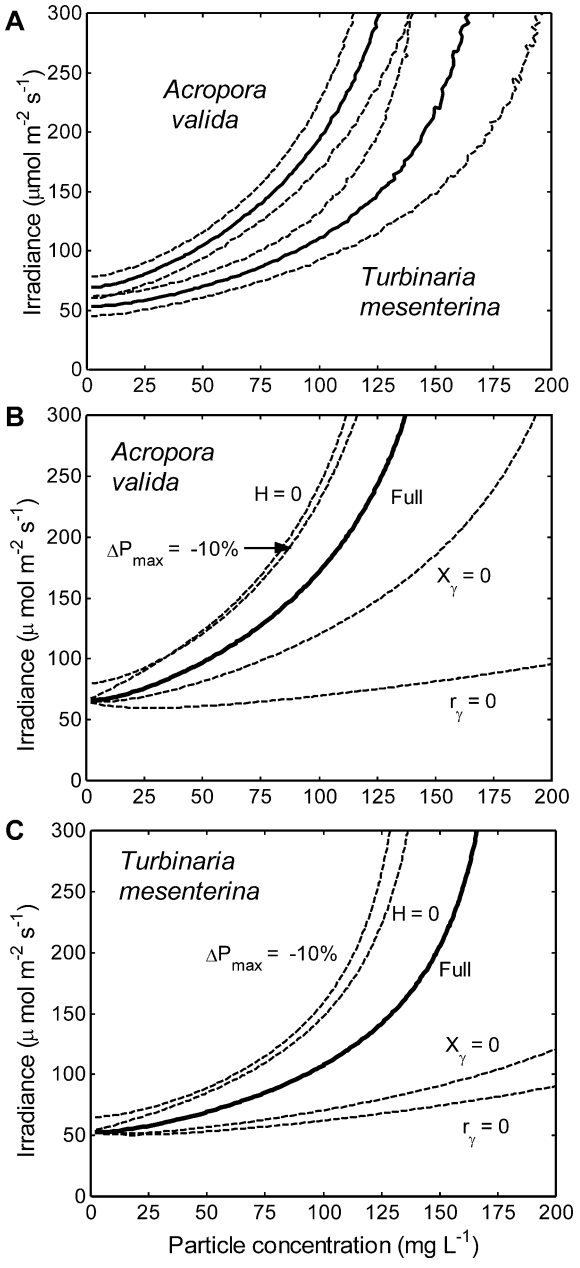

Fig. 2 **a** Zero-growth isoclines (niche boundaries, *solid lines*) for the study species in irradiance-turbidity space. Confidence limits (*dashed lines*) are ±1 standard deviation as determined by Monte Carlo analysis (see Appendix 2). Analyses used parameter values listed in Table 4. **b** Sensitivity of the location of niche boundaries for *A. valida* and (**c**) *T. mesenterina* to variations in the functional responses of energy costs (respiration and organic carbon loss) and energy intakes (photosynthesis and heterotrophy) to particle concentration. *Labels associated with each of the dashed lines* indicate the model parameter value used in each analysis

Consistent with the habitat distributions of the two species, the turbidity-light niche of *T. mesenterina* was substantially larger than that of *A. valida* for most turbidity-irradiance combinations, indicated by the separate locations of their zero-growth isoclines (Fig 2a). That is, *T. mesenterina* is predicted to be able to maintain a positive energy balance in lower light, and higher turbidity, than *A. valida*. Interestingly, for particle concentrations approaching 0 mg l^{-1}, the zero-growth isoclines of the two species converged towards an irradiance intercept of around 60–70 μmol photons m^{-2} s^{-1}, representing the minimal light requirement under clear-water conditions.

In both species, the location of niche boundaries was highly sensitive to variation in turbidity-enhanced respiration (denoted by the parameter R_γ) and to a lesser degree to variation in turbidity-enhanced rates of organic carbon loss (parameter L_γ). This was indicated by the isocline for the scenario R_γ=0 (Fig. 2b, c) being located the furthest from the isocline for the full model. The isocline for the scenario L_γ=0 showed stronger divergence from the full model in *T. mesenterina* than in *A. valida*, indicating that turbidity-enhanced carbon loss is relatively more important in *T. mesenterina*. Interestingly, niche boundaries were nearly identical for the two species in the R_γ=0 case, indicating that species-specific differences in the respiration response to turbidity explained almost all of the interspecific difference in niche-boundary locations.

The location of turbidity niche boundaries was far less sensitive to variations in heterotrophy (represented by maximum versus minimum heterotrophic capacity) than to either of the turbidity-enhanced energy-cost functions. In both species, the effect of eliminating particle feeding capacity was much smaller than that of eliminating functional responses to respiration or organic carbon loss. Indeed, the heterotrophy response was similar in magnitude to a reduction in photosynthetic capacity (denoted by the parameter P_{max}) of only 10% (Fig. 2b, c).

Discussion

In environments characterized by resource limitation or stressors that increase maintenance costs, species may live close to their thresholds for growth and survival—i.e. close to the boundaries of their fundamental niches. In such habitats, mechanisms for minimizing energy expenditure on maintenance and stress tolerance, as well as mechanisms for maximizing the efficiency of energy intake from limiting resources, may be critical for sustaining a positive energy balance. The framework of energy balance models, or scope for growth, has been used previously to formulate theories about how individuals and populations respond to environmental variables (Calow and Sibly 1990; Calow and Forbes 1998; Maltby 1999). For example, Porter (1976) proposed that Caribbean coral species were partitioned along axes of light and zooplankton availability according to their heterotrophic and autotrophic capacities. However, most models of organism energetics in varying resource environments have focused primarily on the functional responses of energy intakes and have assumed that energy costs are mainly functions of organism size or age (e.g. Sebens 1982; Kooijman 2000; Nisbet et al. 2000). Although it is well established that metabolic cost varies with organism activity and environmental regime (e.g. Withers 1992), only a few studies have formally analyzed energy costs as

functional responses of environmental variables, and most have focused on toxicological responses rather than responses to resource availability (e.g. see review by Maltby 1999). The present study extends that approach to environmental variables that act simultaneously as resources and stressors, using their effects on niche boundaries as a common currency with which to assess their importance as determinants of ecological distribution.

A key result of this study is that the functional response characteristics of energy costs are as important as those of energy intakes in determining the location of niche boundaries. For the particular species used here (*A. valida* and *T. mesenterina*), differences in the functional response of respiration to turbidity explain nearly all of the apparent difference in the size of physiological niches. This indicates that assumptions of constant energy losses in relation to resource-stress variables can substantially bias estimates of the absolute and relative locations of a species' niche boundaries, and thus complicate attempts to explain the ecophysiological basis of species-specific differences in ecological distributions.

Variation in heterotrophic capacity (H) produced a relatively minor shift in the location of niche boundaries, supporting inferences drawn in previous studies (Anthony and Fabricius 2000). Given that our values for assimilation efficiency, proportion of time spent feeding and organic carbon content of the suspended particles were all set high, the energy contribution from particle heterotrophy is overestimated. These results suggest that any partitioning of species along axes of light and food availability is unlikely to be driven by differences in heterotrophic capacity as hypothesized by Porter (1976). In contrast, the location of niche boundaries was highly sensitive to reductions in photosynthetic capacity (P_{max}), for example as a consequence of reductions in symbiont density (bleaching). Indeed, for both species, reducing phototrophy by only 10% had an effect similar in magnitude to that of completely omitting heterotrophy from the energy balance.

The functional responses of respiration and organic carbon loss were linear over a range of turbidities (1–200 mg l^{-1}) that encompasses those recorded in most previous studies of turbidity on coral reefs (e.g. Rogers 1990; Larcombe et al. 2001). This was surprising because we expected rates of respiration and organic carbon loss to reach a plateau at high turbidities as individuals reached limits to metabolic rate or gas exchange and mucus production. Moreover, because metabolic rate in anthozoans is directly related to the oxygen gradient within the boundary layer (Patterson and Sebens 1989; Shick 1991), sediment deposition onto coral tissues may present a barrier to oxygen flux and hence reduced respiration at high turbidities. The observed linear responses of respiration rate thus suggest that physiological activities associated with handling turbidity stress (e.g. sediment cleaning) in nature do not represent a maximum load on the system, at least not at the (moderate) temperature (26–27°C) and flow environment (~5 cm s^{-1}) of these experiments.

This study uses physiological niche boundaries (modelled as zero energy balance isoclines) to quantify and compare the ecological importance of different metabolic functional responses along two key environmental gradients for reef corals. The results show that functional responses of energy costs are important determinants of species distributions along these gradients. Indeed, nearly 100% of the difference in physiological niche boundaries of the inshore *T. mesenterina* and the generalist *A. valida* can be attributed to the fact that respiration increases more steeply with turbidity in the latter than in the former. This result contrasts markedly with previous explanations for differences in habitat distributions of corals, which have tended to emphasize putative differences in photosynthetic and heterotrophic parameters (e.g. Porter 1976; Anthony and Fabricius 2000). Like light and turbidity for reef corals, many resources are likely to impose metabolic costs, particularly when their supply rates are high (e.g. photodamage and nutrient toxicity in plants). Therefore, we propose that the functional responses of energy-cost processes should become an integral part of the theoretical framework within which we interpret niche differences and niche partitioning in ecological systems.

Acknowledgements This study was funded by the Australian Research Council (grant No. A00105071 to K.R.N.A. and grant No. DP0209047 to S.R.C. and LP0453612 to the CCRB) and a JCU Merit Research Grant. We thank Tove Lemberget, Liz Madin, Pia Rheinlander, and Tim Prior for their assistance in the laboratory, Michael Bode for help with the MATLAB code for Monte Carlo analyses, and to the Australian Institute of Marine Science for use of the CHN analyzer. This is contribution number 81 from the Centre for Coral Reef Biodiversity.

Appendix 1

Rate of photosynthesis versus average daily irradiance

To test the efficacy of using average irradiance during the day rather than irradiance-time profiles in our calculations of daily rates of photosynthesis, we compared the outputs of these two methods for 12 days with varying maximum (1200 hours) irradiances (I_{noon}, 10–1,500 μmol m^{-2} s^{-1}). Method 1 used a traditional irradiance sine function with a 12-h day length as input [$I_t = I_{noon} \sin(t\pi/12)$, where I_t is irradiance averaged over a 1-h window and t is hours since sunrise], whereas method 2 used the average daily irradiance (I) as input. Daily gross rate of photosynthesis for method 1 was calculated as

$$P_{g1} = \sum_{t=0}^{12} P_{max} \tanh \frac{I_t}{I_k}, \tag{10}$$

and for method 2 as

$$P_{g2} = 12 P_{max} \tanh \frac{I}{I_k}, \tag{11}$$

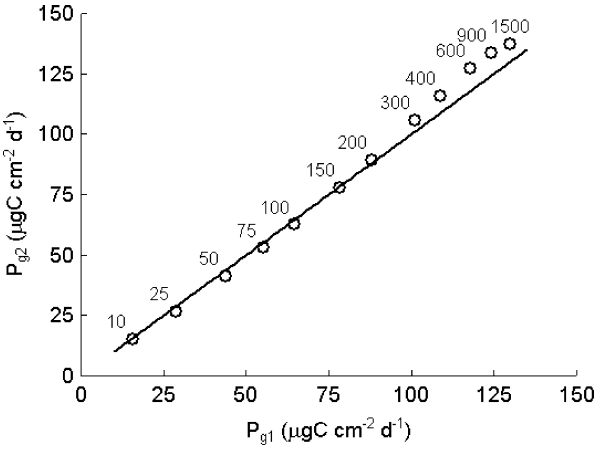

Fig. 3 Plotting of P_{g2} against P_{g1} indicates negligible bias from the unity line

Table 5 Variance–covariance matrices for photosynthesis and respiration (A) and organic carbon loss parameters (B) for *A. valida* and *T. mesenterina*. See Table 4 for a summary of parameter means. Note that variances and covariances for β_1 and β_2 (the acclimation responses of P_{max} and I_k to changing growth irradiances) were unavailable, so we used the mean values presented in Table 4 for those parameters. Also, because most of the parameters for heterotrophy ($\gamma_{sat,\ \varepsilon\ \tau}$ and c_{org}) were fixed at (high) values, variation in heterotrophy was simulated using only the variance in maximum feeding rate, F_{max}

	T. mesenterina				*A. valida*			
	P_{max}	I_k	R_{base}	R_γ	P_{max}	I_k	R_{base}	R_γ
A. Photosynthesis and respiration								
P_{max}	51.71	69.60	11.92	7.90	2.30	15.19	0.52	0.25
I_k	69.60	338.32	−13.19	10.75	15.19	339.98	−4.24	3.73
R_{base}	11.92	−13.19	16.82	−14.02	0.52	−4.24	0.78	−0.60
R_γ	7.90	10.75	−14.02	73.14	0.25	3.73	−0.60	2.60

	T. mesenterina			*A. valida*		
	L_{base}	L_γ	L_I	L_{base}	L_γ	L_I
B. Rates of organic carbon loss						
L_{base}	6.48	−4.94	−5.25	0.15	−0.14	−0.10
L_γ	−4.94	14.73	−2.22	−0.14	0.37	−0.04
L_I	−5.25	−2.22	12.43	−0.10	−0.04	0.29

where P_{max} is maximum hourly rate of photosynthesis and I_k is the irradiance at which the rate of photosynthesis is ~75% of maximum. P_{max} and I_k are functions of I according to Eq. 8 (Anthony and Hoegh-Guldberg 2003a). Plotting P_{g2} against P_{g1} indicates negligible bias ($P_{g2} \cong P_{g1}$) for 1200 hours irradiances below 300 µmol m^{-2} s^{-1} (Fig. 3) . Thus, for the low light regimes characteristic of high-turbidity environments, the two methods produce nearly identical estimates of daily rates of photosynthesis.

Appendix 2

Confidence limits of niche boundaries using Monte Carlo analysis

To model energy balance for a given turbidity and irradiance, we used parameter estimates, their statistical variances, and (where applicable) their statistical covariances. We followed standard Monte Carlo procedure, sampling sets of parameter values from the multivariate normal distribution specified by the parameter estimates and their associated variance covariance matrices (Table 5). This procedure was repeated for a range of turbidity (1–200 mg l^{-1}) and irradiance (0–300 µmol m^{-2} s^{-1}) values. The sampling procedure was repeated 1,000 times for each turbidity-irradiance combination, and the standard deviation at each combination used as the confidence limits for the location of zero-E_B isoclines.

References

Acevedo R, Morelock J, Olivieri RA (1989) Modification of coral reef zonation by terrigenous sediment stress. Palaios 4:92–100

Anthony KRN (1999) Coral suspension feeding on fine particulate matter. J Exp Mar Biol Ecol 232:85–106

Anthony KRN, Fabricius KE (2000) Shifting roles of heterotrophy and autotrophy in coral energetics under varying turbidity. J Exp Mar Biol Ecol 252:221–253

Anthony KRN, Hoegh-Guldberg O (2003a) Kinetics of photo-acclimation in corals. Oecologia 134:23–31

Anthony KRN, Hoegh-Guldberg O (2003b) Variation in coral photosynthesis, respiration and growth characteristics in contrasting light microhabitats: an analogue to plants in forest gaps and understoreys? Funct Ecol 17:246–259

Anthony KRN, Ridd PV, Orpin AR, Larcombe P, Lough JM (2004) Temporal variation in light availability in coastal benthic habitats: effects of clouds, turbidity and tides. Limnol Oceanogr (in press)

Barnes DJ, Chalker BE (1990) Calcification and photosynthesis in reef-building corals and algae. In: Dubinsky Z (ed) Ecosystems of the world: coral reefs, vol 25. Elsevier, Amsterdam, pp 109–131

Brose U, Williams RJ, Martinez ND (2003) Comment on foraging adaptation and the relationship between food web complexity and stability. Science 301:918b

Calow P, Forbes VE (1998) How do physiological responses to stress translate into ecological and evolutionary processes. Comp Biochem Phys A 120:11–16

Calow P, Sibly RM (1990) A physiological basis of population processes: ecotoxicological implications. Funct Ecol 4:283–288

Chalker BE, Dunlap WE, Oliver JK (1983) Bathymetric adaptations of reef-building corals at Davies Reef, Great Barrier Reef, Australia. II. Light saturation curves for photosynthesis and respiration. J Exp Mar Biol Ecol 73:37–56

Chazdon RL, Pearcy RW, Lee DW, Fetcher N (1996) Photosynthetic responses of tropical forest plants to contrasting light environments. In: Mulkey SS, Chazdon RL, Smith AP (eds) Tropical forest plant ecophysiology. Chapman and Hall, London, pp 5–55

Chesson P, Huntly N (1997) The roles of harsh and fluctuating conditions in the dynamics of ecological communities. Am Nat 150:519–553

Crossland CJ (1987) In situ release of mucus and DOC-lipid from the coral *Acropora variabilis* and *Stylophora pistillata*. Coral Reefs 6:35–42

Done TJ (1982) Patterns in the distribution of coral communities across the central Great Barrier Reef. Coral Reefs 1:95–107
Done TJ (1983) Coral zonation: its nature and significance. In: Barnes DJ (ed) Perspectives on coral reefs. Australian Institute of Marine Science, Canberra, pp 107–147
Emery NC, Ewanchuk PJ, Bertness MD (2001) Competition and salt-marsh plant zonation: stress tolerators may be dominant competitors. Ecology 82:2471–2485
Falkowski PG, Raven JA (1997) Aquatic photosynthesis. Blackwell, Oxford
Ferrier-Pages C, Allemand D, Gattuso JP, Jaubert J, Rassoulzadegan R (1998) Microheterotrophy in the zooxanthellate coral *Stylophora pistillata*: effects of light and ciliate density. Limnol Oceanogr 43:1639–1648
Gurney WSC, Middleton DAJ, Nisbet RM, McCauley E, Murdoch WM, DeRoos A (1996) Individual energetics and the equilibrium demography of structured populations. Theor Popul Biol 49:344–368
Hutchinson GE (1957) Concluding remarks. Cold Spring Harb Symp Quant Biol 22:415–427
Kooijman SALM (2000) Dynamic energy and mass budgets in biological systems, 2nd edn. Cambridge University Press, Cambridge
Lambers H, Chapin FS III, Pons TL (1997) Plant physiological ecology. Springer, Berlin Heidelberg New York
Larcombe P, Costen A, Woolfe KJ (2001) The hydrodynamic and sedimentary setting of nearshore coral reefs, central Great Barrier Reef shelf, Australia: Paluma Shoals, a case study. Sedimentology 48:811–835
Larcombe P, Ridd PV, Prytz A, Wilson B (1995) Factors controlling suspended sediment on inner-shelf coral reefs, Townsville, Australia. Coral Reefs 14:163–171
Leibold MA (1995) The niche concept revisited: mechanistic models and community context. Ecology 76:1371–1382
Maltby L (1999) Studying stress: the importance of organism-level responses. Ecol Appl 9:431–440
McClanahan TR, Obura D (1997) Sedimentation effects on shallow coral communities in Kenya. J Exp Mar Biol Ecol 209:103–122
Muscatine L (1990) The role of symbiotic algae in carbon and energy flux in reef corals. In: Dubinsky Z (ed) Ecosystems of the world: coral reefs, vol 25. Elsevier, Amsterdam, pp 75–87
Nisbet RM, Muller EB, Lika K, Kooijman SALM (2000) From molecules to ecosystems through energy budget models. J Anim Ecol 69:913–926
Ohmann JL, Spies TA (1998) Regional gradient analysis and spatial pattern of woody plant communities of Oregon forests. Ecol Monogr 68:151–182
Patterson MR, Sebens KP (1989) Forced convection modulates gas exchange in cnidarians. Proc Natl Acad Sci USA 86:8833–8836
Porter JW (1976) Autotrophy, heterotrophy, and resource partitioning in Caribbean reef-building corals. Am Nat 110:731–742
Riegl B, Branch GM (1995) Effects of sediment on the energy budgets of four scleractinian (Bourne 1900) and five alcyonacean (Lamouroux 1816) corals. J Exp Mar Biol Ecol 186:259–275
Rogers CS (1990) Responses of coral reefs and reef organisms to sedimentation. Mar Ecol Prog Ser 62:185–202
Seabloom EW, Moloney KA, van der Valk AG (2001) Constraints on the establishment of plants along a fluctuating water-depth gradient. Ecology 82:2216–2232
Sebens KP (1982) Limits to indeterminate growth: an optimal size model applied to passive suspension feeders. Ecology 63:209–222
Sebens KP (1987) The ecology of indeterminate growth in animals. Annu Rev Ecol Syst 18:371–407
Shick JM (1991) A functional biology of sea anemones. Chapman and Hall, London
STATISTICA (2001) STATISTICA (data analysis software system), version 6. StatSoft, Tulsa
Sultan SE, Bazzaz FA (1993) Phenotypic plasticity in *Polygonum persicaria*. III. The evolution of ecological breadth for nutrient environment. Evolution 47:1050–1071
Veron JEN (1986) Corals of Australia and the Indo-Pacific, 2nd edn. University of Hawaii Press, Honolulu
Withers PC (1992) Comparative animal physiology. Saunders College, Fort Worth